J Neurol (2002) 249 : 1382–1390
DOI 10.1007/s00415-002-0846-6

ORIGINAL COMMUNICATION

Choline is increased in pre-lesional normal appearing white matter in multiple sclerosis

M. C. Tartaglia
S. Narayanan
N. De Stefano
R. Arnaoutelis
S. B. Antel
S. J. Francis
A. C. Santos
Y. Lapierre
D. L. Arnold

Abstract *Objective* Our aim was to determine if the resonance intensity of choline-containing compounds (Cho) measured using proton magnetic resonance spectroscopy (MRS) was increased in pre-lesional normal appearing white matter (NAWM) in patients with multiple sclerosis (MS) relative to NAWM that remained stable in subsequent scans. *Background* The Cho peak in MR spectra is associated with membrane phospholipids and increases in acute MS plaques, possibly even before the appearance of MRI-visible MS lesions. *Methods* Three combined proton MRI and MRS imaging examinations of the corpus callosum and adjacent periventricular white matter were performed on 12 MS patients at intervals of 6 months. Proton density (PD) images were visually matched across 3 time points and the lesion volume in each voxel of the volume of interest was determined. The voxels were subdivided into four groups based on the presence or absence of lesion at baseline and change or no change in lesion volume on the subsequent scan. *Results* We found a significantly higher baseline Cho/Creatine (Cr) ratio in NAWM voxels that displayed MRI visible lesions 6 months later than NAWM voxels that remained unchanged (1.57 ± 0.30 and 1.37 ± 0.33, respectively, $p < 0.001$). The 12-month interval data revealed similar pre-lesional elevated Cho/Cr, (1.51 ± 0.29 versus 1.39 ± 0.32, $p = 0.009$). Voxels that contained lesion at baseline and increased in lesion volume at 6 months also showed a significantly higher Cho/Cr ratio than those whose lesion volume did not change (1.60 ± 0.32 and 1.49 ± 0.36, respectively, $p = 0.043$). *Conclusions* The results of this study are consistent with focal pre-lesional myelin membrane pathology in the NAWM at least 12 months before lesions become visible on conventional MRI. This could reflect altered myelin chemistry or the presence of inflammation as seen in experimental allergic encephalomyelitis.

Key words multiple sclerosis · choline · magnetic resonance spectroscopy · normal appearing white matter

Received: 26 November 2001
Received in revised form: 13 March 2002
Accepted: 15 April 2002

M. C. Tartaglia, BSc · S. Narayanan, MSc · R. Arnaoutelis, BSc · S. B. Antel, MSc · S. J. Francis, BSc · A. C. Santos, MD, PhD · Y. Lapierre, MD · D. L. Arnold, MD (✉)
Magnetic Resonance Spectroscopy Unit
Montreal Neurological Institute
3801 University Street
Montreal, Quebec, H3A 2B4, Canada
Tel.: +1-514/398-8185
Fax: +1-514/398-2975
E-Mail: doug@mrs.mni.mcgill.ca

N. De Stefano, MD, PhD
Institute of Neurological Sciences & NMR Centre
University of Siena, Italy

Introduction

Multiple sclerosis (MS) is an idiopathic demyelinating disease characterized by the formation of plaques located primarily in the white matter. These lesions are readily visible as hyperintensities on T2-weighted (T2W) and proton density-weighted (PD) magnetic resonance images (MRI) and are believed to represent a variable combination of demyelination, inflammation and axonal loss [17, 27]. In an effort to better understand the pathophysiology of MS, proton magnetic resonance spectroscopy (^{1}H-MRS) has been used to measure non-invasively the metabolic changes in the brains of MS patients [2, 3, 14, 16, 22, 28]. The metabolites most amenable to study with ^{1}H-MRS are N-acetylaspartate (NAA), choline (Cho) and creatine (Cr). The most intense resonance is visible at 2.0 ppm, and corresponds to

N-acetyl groups, which originate mainly from N-acetyl-aspartate. The NAA signal has been used as a marker of neuronal integrity because it is localized to neurons and neuronal processes in the mature brain [26]. The ratio of NAA/Cr has been reported to decrease in demyelinating plaques as well as in the normal appearing white matter (NAWM) on conventional MRI of MS patients [3]. Creatine-containing compounds are seen at 3.0 ppm. Creatine is relatively homogeneously distributed throughout the brain; thus it has been used as an internal reference peak to calculate NAA/Cr and Cho/Cr ratios [1]. It must, however, be noted that there is inconsistency in reports of quantification of creatine [5, 11, 20, 24, 25, 29]. In an *in vitro* study, a decrease of creatine was noted only in MS plaques, while most of the NAWM remained unchanged [5, 29]. Choline-containing compounds can be observed at 3.2 ppm. The Cho peak is believed to represent a combination of free choline, phosphorylcholine, glycerylphosphorylcholine, and possibly taurine and betaine [4].

The pathological significance of changes in choline levels in the central nervous system is unclear. The compounds responsible for the choline peak are associated with membrane phospholipids and have been reported to increase in acute stage plaques, when active demyelination and inflammation are occurring [2, 3]. In acute experimental allergic encephalomyelitis (EAE), however, an increase in Cho/Cr peaks was associated only with inflammation and was due to the presence of lymphocytes [4]. In the acute stage of EAE, there is mainly inflammation with little or no demyelination. 1H-MRS performed on patients with brain tumors or brain infectious diseases revealed that cellular density and water-soluble choline-containing compounds were the best determinants of the Cho/Cr peak [9, 15].

Using Magnetization Transfer (MT) techniques, a number of laboratories have demonstrated a decreased MT in brain areas that subsequently develop MRI-visible plaques [7, 8, 21]. We speculated that membrane disruption and/or inflammation occurring in the NAWM prior to the development of MRI-visible plaques might be observed as an increase in Cho/Cr ratios in that area [3]. Narayana et al. [18] reported a localized increase of Cho in two patients who subsequently developed a MRI-visible plaque at those sites. The purpose of this study was to acquire proton MRS data from MS patients and determine if increases in choline levels in the NAWM could be used to differentiate areas that would develop plaque from those that remained stable in subsequent scans.

Methods

Patients

Twelve patients with definite MS (7 women and 5 men) were recruited via the MS clinic at the Montreal Neurological Institute and Hospital. The group included 7 relapsing-remitting (RR) patients and 5 secondary progressive (SP) patients. The group had a mean Expanded Disability Status Scale (EDSS) of 4.54 ± 2.3 at Time Point 1, ($RR_{mean} = 3$, $SP_{mean} = 6.7$) and their mean age was 43.98 ± 9.7 years (range = 34.7–61.2). Twenty-nine normal controls were recruited from hospital staff and friends. Their mean age was 34.12 ± 8.7 years (range = 26.3–57.1). The Ethics Committee of the Montreal Neurological Institute and Hospital approved the study and informed consent was obtained from all participants. The patients' demographic data are given in Table 1.

Data acquisition

Proton MRI/MRSI

Combined proton MRI and MRSI examinations of the brain were performed using a Philips Gyroscan ACS operating at 1.5 T (Philips Medical Systems, Best, the Netherlands). A transverse dual-echo, turbo spin-echo sequence (TR/TE1/TE2 = 2075/32/90 ms, 256×256 matrix, 1 signal average, 250mm field of view) yielding proton density-weighted (PDW) and T2-weighted (T2W) images with 50 contiguous 3 mm slices was acquired parallel to the plane connecting the anterior and posterior commissures (AC-PC line). This was followed by a matching T1-weighted (T1W) fast field-echo (FFE) sequence (TR/TE = 35/10 ms). These MR images were used to position a spec-

Table 1 Patient demographics and individualized imaging data as well as means for each parameter at the three time points.

Patient	Sex	Age	Type	EDSS 1, 2, 3	Lesion Vol 1, 2, 3 (cm^3)	Disease duration at entry (years)	NAA/Cr 1, 2, 3	Cho/Cr 1, 2, 3
1	M	61.2	SP	6.5, 6.5, 6.5	8.52, 8.64, 10.01	25.6	2.90, 3.13, 2.74	1.53, 1.55, 1.42
2	M	36.6	RR	0.0, 2.0, NA	2.69, 4.02, NA	0.9	2.98, 2.83, NA	1.59, 1.44, NA
3	F	46.3	RR	4.5, 4.5, 5.5	0.91, 1.30, 2.91	15.6	2.39, 2.42, 2.55	1.31, 1.35, 1.45
4	F	35.5	RR	3.5, 2.5, 2.0	7.76, 9.09, 10.37	6.6	2.53, 2.58, 2.60	1.51, 1.52, 1.42
5	F	56.7	SP	8.0, 8.0, NA	8.21, 7.84, NA	37.0	2.66, 2.55, NA	1.35, 1.28, NA
6	F	35.8	RR	2.5, 2.5, 2.5	4.75, 5.81, 3.97	13.3	2.64, 2.80, 2.73	1.53, 1.61, 1.63
7	M	48.1	SP	7.0, 7.0, NA	1.23, 0.94, NA	18.0	2.88, 2.86, NA	1.33, 1.28, NA
8	F	57.4	RR	3.5, 3.0, NA	10.6, 11.3, NA	22.2	2.84, 2.50, NA	1.19, 1.14, NA
9	F	36.3	SP	6.0, 6.5, 6.5	4.27, 7.68, 6.08	12	2.88, 2.72, 2.82	1.90, 1.62, 1.79
10	F	38.9	RR	3.0, 3.0, 3.5	2.72, 3.25, 3.93	10.7	2.56, 2.71, 2.47	1.32, 1.39, 1.38
11	M	40.1	RR	4.0, 4.0, 4.0	7.84, 8.62, 7.13	19.8	2.64, 2.50, 2.68	1.31, 1.25, 1.28
12	M	34.7	SP	5.5, 6.0, 6.0	11.1, 8.75, 8.91	13.1	2.59, 2.68, 2.56	1.44, 1.50, 1.36
Mean		**43.98**		**4.5, 4.6, 4.6**	**5.88, 6.44, 6.66**	**16.23**	**2.71, 2.69, 2.64**	**1.44, 1.41, 1.47**

troscopic volume of interest (VOI) of approximately 90×90×20 mm^3 to include the corpus callosum and adjacent periventricular white matter. This VOI includes approximately 121 voxels with a nominal volume of 1.28 cm^3 each. All voxels at the edges of the VOI were excluded because of potential chemical shift artifacts on the relative amplitudes thus leaving a maximum of 100 voxels per patient for analysis. The number of PDW images corresponding to the spectroscopic VOI and inspected for lesions varied between 6 and 7 but remained constant in an individual across the different scans. MR spectroscopic images parallel to the AC-PC line were acquired (32×32 phase-encodes, 250×250 mm field-of-view, 20 mm slab thickness) using a double spin-echo excitation method (TR 2000, TE 272ms) [19]. Suppression of the intense water resonance was accomplished by placing frequency selective excitation pulses at the beginning of the MRSI sequence. To allow for correction of B_0 inhomogeneity during post-processing, a quick MRSI without water-suppression was also acquired (TR 850ms, TE 272ms, 16×16 phase-encodes, 250×250 mm field-of-view and one signal average) [6].

Post-Processing

Metabolite resonance intensities were determined using a combination of XunSpec1 (Philips, the Netherlands) and locally-developed software (AVIS, Samson Antel, MRS Unit, Montreal Neurological Institute) which integrates fitted peak areas between automatically determined frequency bounds relative to a locally interpolated baseline. Metabolite signals are expressed as ratios to Cr in the same voxel.

Image Data analysis

Three serial scans taken at six-month intervals over 12 months were used in this study. The PD images corresponding to the spectroscopic VOI were inspected visually for lesion volumes. The lesion fraction in each voxel was determined by assigning a value of 0, 0.125, 0.25, 0.5, 0.75 or 1 depending on the percentage of lesion occupying that voxel in 1 PD image. The process was repeated for all the PD images corresponding to the spectroscopic box. The mean lesion fractions were then added up and multiplied by the nominal volume (1.28 cm^3) contained in each spectroscopic voxel. This process was done for the three time points independently.

In order to determine the changes in lesion load over time in a given voxel, PD images with the overlaid spectroscopic phase-encoding grid were visually matched across the three time points (Fig. 1). Two 12-month scans had to be eliminated because the images with their corresponding voxels could not be matched to previous scans. An additional two 12-month scans had to be rejected because of incorrect voxel size. Therefore, a total of 12 scans were included for the 6-month interval analysis but only eight scans were retained for the 12-month interval analysis. All the spectroscopic data was assessed for quality and adequacy of fit. Any voxel without a corresponding voxel in any of the subsequent scans was rejected. Furthermore, voxels that contained lesion that regressed over time were also excluded from this analysis. A total of 604 voxels for the 6-month interval and 414 voxels for the 12-month interval were retained for analysis. The voxels retained were then subdivided into four groups depending on the presence or absence of lesion at Time Point 1 (TP1) and change or

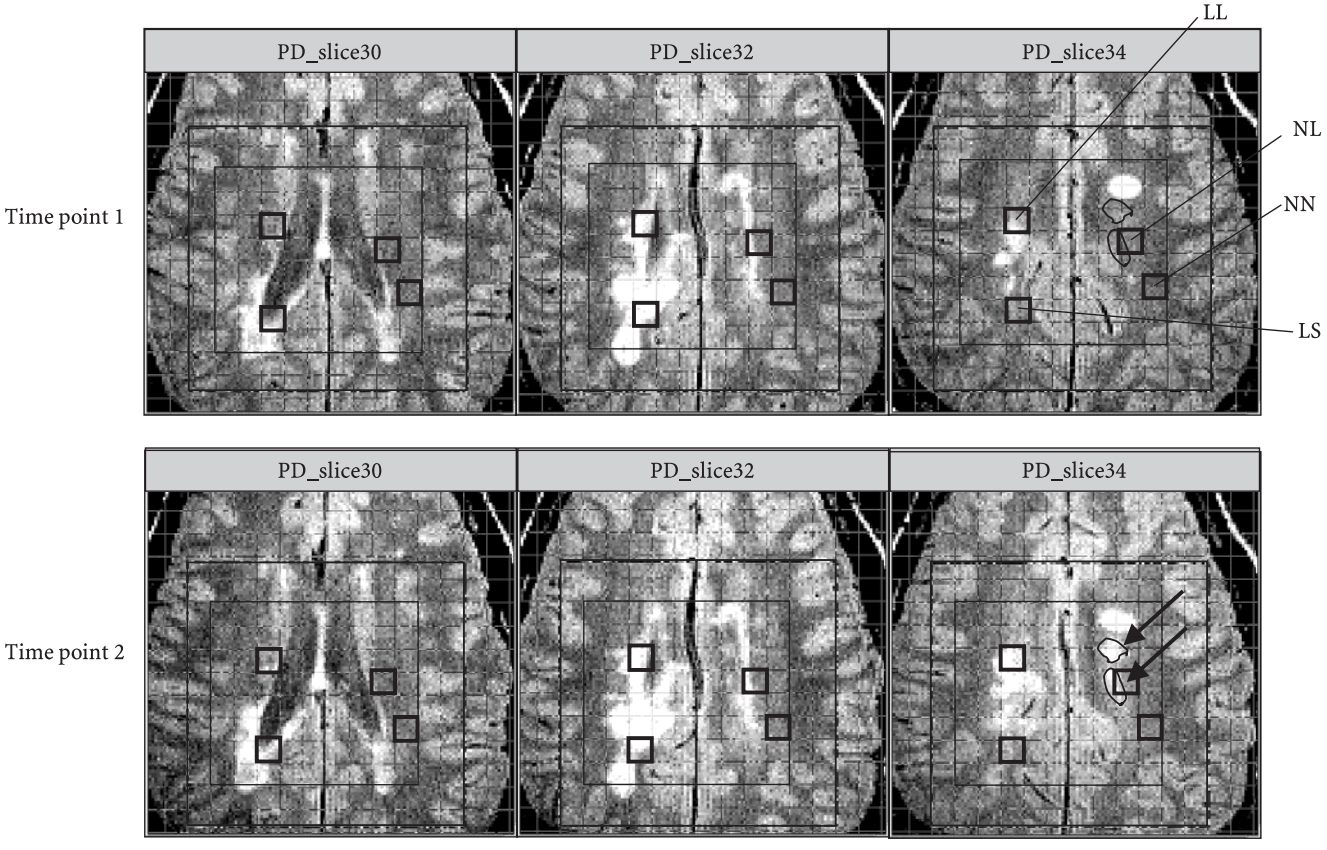

Fig. 1 Proton density (PD) images corresponding to the spectroscopic box were visually matched across the 3 time points. Seen here are PD Images from an RR patient at TP1 and TP2. Arrows indicate new lesion areas. Box *NL* refers to NAWM voxels that displayed a new lesion in the subsequent scan. Box *NN* refers to voxels of NAWM that remain as NAWM in the subsequent scan. Box *LL* refers to voxels with lesion that had increased in size by the subsequent scan. Box *LS* refers to voxels with lesions that had remained stable at the subsequent scan.

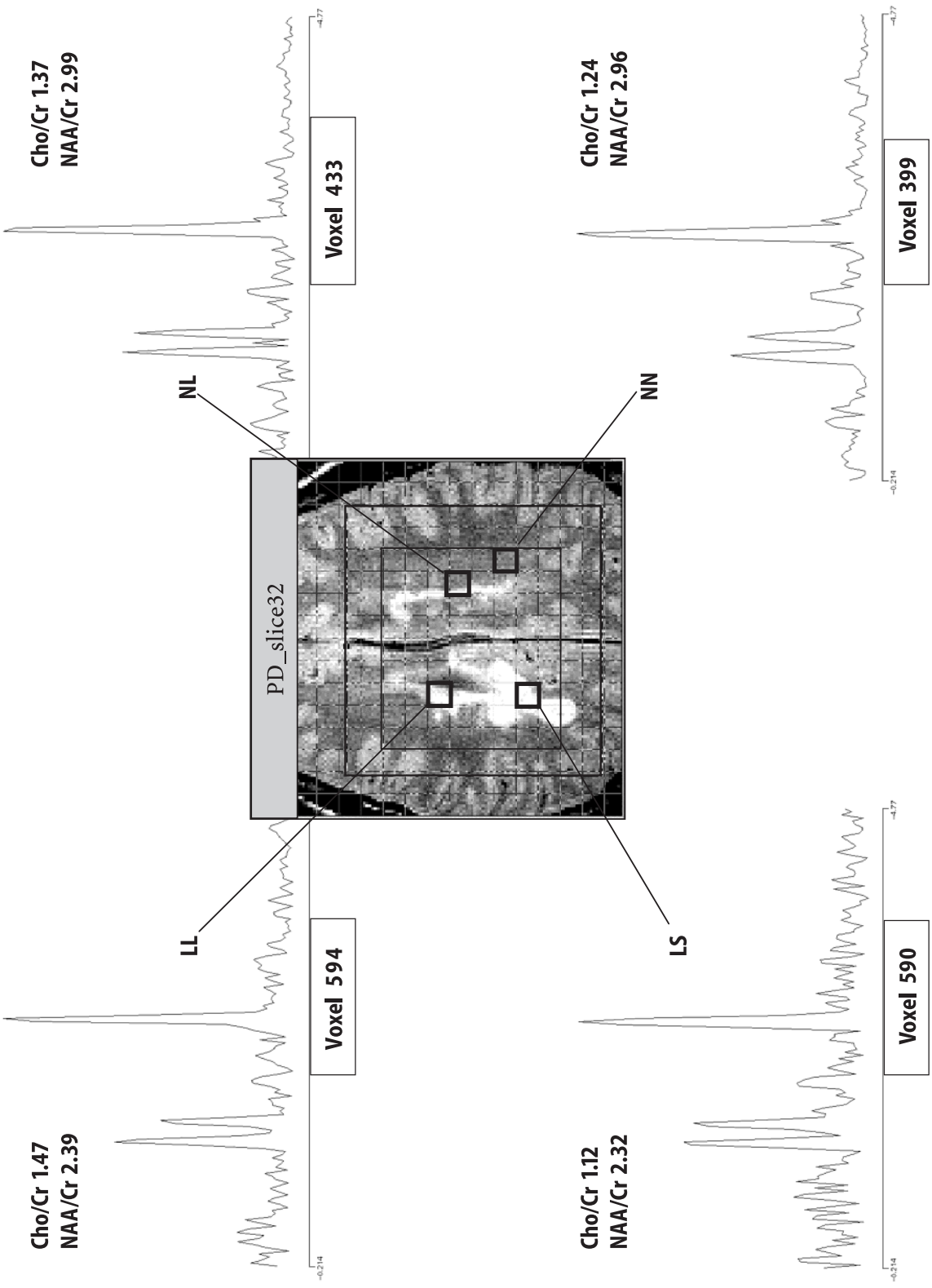

Fig. 2 A Proton density image from the same RR patient seen in Fig. 1 at Time point 1 with examples of spectroscopic data for the 6-month interval analysis from the NL, NN, LL and LS groups.

no change in lesion volume on the subsequent scan. The four groups are: Group NN: NAWM-NAWM, voxels of NAWM at TP1 that remained as NAWM on a subsequent scan, Group NL: NAWM-LESION, voxels of NAWM at TP1 in which a lesion appears on a subsequent scan, Group LS: LESION-STABLE, voxels containing lesion at TP1 with no change in lesion volume on subsequent scan, Group LL: LESION-LESION, voxels containing lesion at TP1 with increase in lesion volume on subsequent scan. The 6-month analysis included 364 voxels in Group NN, 62 voxels in Group NL, 77 voxels in Group LS, and 101 voxels in Group LL (Fig. 2). The 12-month analysis included 221 voxels in Group NN, 56 voxels in Group NL, 67 voxels in Group LS, and 70 voxels in Group LL.

In order to determine the temporal stability of MRSI data, we assessed reproducibility of repositioning and metabolite ratios in 6 normal subjects who were scanned twice.

Statistical Analysis

Two-sample t-tests were performed to compare patients' metabolite ratios between lesion containing voxels and NAWM at each time point. They were also used to compare metabolite ratios within the two Lesion groups and within the two NAWM groups. A Mann-Whitney U test was used in the analysis of the individual patients' data. An Analysis of Variance (ANOVA) with Bonferroni correction was used to establish any significant differences in metabolite ratios between control, NAWM and Lesion voxels. Pearson correlation tests were used to examine the relationship between metabolite ratio and the amount of lesion in each voxel. A Spearman rank coefficient was used to determine correlation in the small samples. All statistical analyses were performed using SYSTAT 9.0.

Results

Reproducibility

Six of the controls in this study were scanned twice to assess the reproducibility of our data. The scan intervals ranged from 0.05 to 2.1 years. The mean difference between the two scans was 3.90 % (range 0.6–8.6 %) for Cho/Cr ratios and 5.36 % (range 0.3–11.9 %) for NAA/Cr.

Patients' demographic data

As can be seen in Table 1, these patients showed no significant change in EDSS scores over time. The lesion volumes also remained fairly constant as well as their mean NAA/Cr and Cho/Cr. We assessed if the lesion volume was significantly different between the two Lesion voxel groups and found that Group LL had a non-significantly higher lesion volume than Group LS at TP1, ($0.201 \pm 0.13\,cm^3$ and $0.166 \pm 0.17\,cm^3$, respectively, $p = 0.135$). The patients in this study were clinically stable; only three patients had an attack in the course of the study and these were at least three months prior to or after a scan.

Controls versus patients

Twenty-nine control subjects were included in this study. An ANOVA with Bonferroni correction revealed a significantly lower Cho/Cr level in voxels of normal control subjects ($N = 2154$) compared with Lesion voxels ($N = 178$) in MS patients (1.45 ± 0.31 and 1.55 ± 0.34, respectively, $p = 0.002$). There was no significant difference in Cho/Cr between NAWM voxels in normal control subjects and NAWM voxels ($N = 426$) in MS patients, (1.45 ± 0.31 and 1.40 ± 0.33, respectively, $p = 0.575$). The NAA/Cr of control subjects was significantly higher than the NAA/Cr ratio in both NAWM and Lesion voxels of MS patients, [3.24 ± 0.52 versus 2.77 ± 0.43 ($p < 0.001$) and 2.66 ± 0.38 ($p < 0.001$), respectively].

NAWM versus Lesion voxels

Cho/Cr was significantly higher in Lesion voxels compared with NAWM voxels at all three Time Points [TP1: 1.55 ± 0.34 ($N = 178$) and 1.40 ± 0.33 ($N = 426$), respectively, $p < 0.001$, TP2: 1.51 ± 0.29 ($N = 229$) and 1.36 ± 0.31 ($N = 375$), respectively, $p < 0.001$, TP3: 1.53 ± 0.30 ($N = 137$) and 1.42 ± 0.33 ($N = 277$), respectively, $p < 0.001$].

NAA/Cr was significantly lower in Lesion voxels than in NAWM voxels at TP1 (2.77 ± 0.43, 2.66 ± 0.38, respectively, $p = 0.002$) and at TP3 (2.67 ± 0.42 and 2.59 ± 0.35, respectively, $p = 0.038$). At TP2, the NAA/Cr although higher in the NAWM voxels than Lesion voxels was not significantly different (2.72 ± 0.45 and 2.68 ± 0.43, respectively, $p = 0.202$).

Correlation between metabolites and lesion volume

There was no significant correlation between Cho/Cr and the lesion volumes within each spectroscopic voxel at TP1 ($r = 0.071$, $p = 0.080$). There was a significant correlation between NAA/Cr values and lesion volume at TP1 ($r = -0.168$, $p < 0.001$).

Choline at 6-month interval

Cho/Cr was significantly higher at TP1 in NAWM voxels that developed lesions at TP2 versus NAWM voxels that remained stable (1.57 ± 0.30 and 1.37 ± 0.33, respectively, $p < 0.001$) (Table 2 and Fig. 3a). Looking at the patients individually, there was a general trend for voxels that went on to develop lesion at TP2 to display an elevated Cho/Cr compared with voxels in the same scan that did not, though in most cases this was not significant owing to the small sample numbers. The levels of Cho/Cr in the voxels of NAWM that went on to develop

Table 2 Descriptive and inferential statistics for the NAWM and LESION groups with respect to Cho/Cr and NAA/Cr at 6 month and 12 month intervals. Sample size, means and standard deviations are shown.

Group	N voxels	Cho/Cr at 6-month	p =	NAA/Cr at 6-month	p =	N voxels	Cho/Cr at 12-month	p =	NAA/Cr at 12-month	p =
NL: Voxel with NAWM that becomes lesion	62	1.57 ± 0.30	< 0.001	2.79 ± 0.35	0.720	56	1.51 ± 0.29	0.009	2.70 ± 0.33	0.491
NN: Voxel with NAWM that remains NAWM	364	1.37 ± 0.33		2.77 ± 0.44		221	1.39 ± 0.32		2.67 ± 0.38	
LL: Voxel with lesion that increases in size	101	1.60 ± 0.32	0.043	2.66 ± 0.38	0.981	70	1.61 ± 0.31	0.408	2.60 ± 0.35	0.742
LS: Voxel with lesion that remains stable	77	1.49 ± 0.35		2.66 ± 0.39		67	1.57 ± 0.34		2.62 ± 0.40	
TOTAL	604					414				

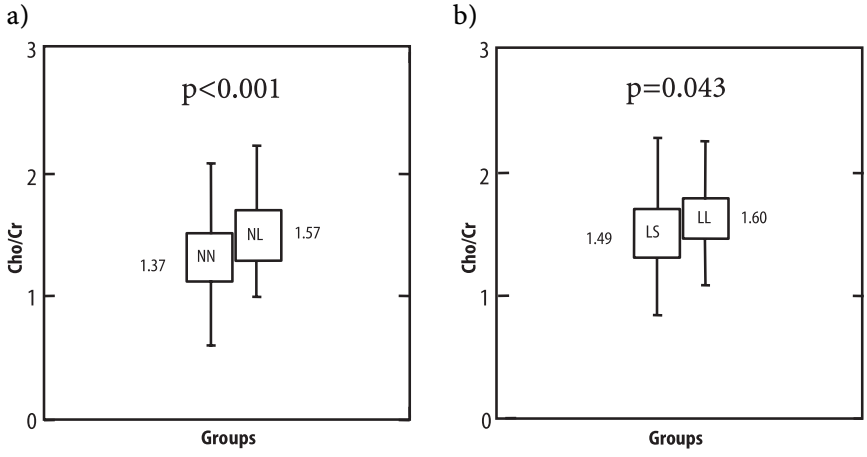

Fig. 3 **a**) Comparing NAWM Groups (NL vs. NN) for Cho/Cr reveals a significantly higher Cho/Cr in NAWM voxels that display a lesion at the 6-month scan (NL: 1.57 ± 0.30 vs. NN: 1.37 ± 0.33, p < 0.001). **b**) Comparing Lesion Groups (LL vs. LS) for Cho/Cr reveals a significantly higher Cho/Cr in Lesion voxels that display an increase in lesion load at the 6-month scan (LL: 1.60 ± 0.32 vs. LS: 1.49 ± 0.36, p = 0.043).

lesions in subsequent scans was 13 % (0.7–27 %) higher than in the voxels that remained stable.

Lesion voxels at TP1 that showed an increase in lesion content on the 6-month scan also had a significantly higher Cho/Cr than Lesion voxels that remained stable, (1.60 ± 0.32 and 1.49 ± 0.36, respectively, p = 0.043) (Table 2 and Fig. 3b). Within each individual scan at TP1, there was no discernable trend towards a higher Cho/Cr ratio in voxels that accrued lesion at TP2 versus those that did not.

NAA at 6-month interval

Neither the NAWM groups (NN, NL) nor the Lesion groups (LS, LL) showed significant differences within the groups for NAA/Cr ratios (Table 2). Although NAA/Cr values were consistently lower in voxels with lesion, there was considerable overlap.

Choline at 12-month interval

We also found a significant difference in Cho/Cr ratios at TP1 between NAWM voxels that remained stable and those that displayed lesions at TP3 (1.39 ± 0.32 and 1.51 ± 0.29, respectively, p = 0.009) (Table 2). In looking at the individual patients, six out of the seven patients displayed elevated Cho/Cr in voxels that went on to develop lesions at TP3, though once again these were for the most part not significantly different because of the small sample numbers. The levels of Cho/Cr in the voxels of NAWM that showed lesions at 12 months were between 7 and 29 % higher than the voxels that remained stable.

In contrast to the 6-month interval data, the two Lesion groups did not show significantly different Cho/Cr ratios, (Group $LL_{mean} = 1.61 \pm 0.31$, Group $LS_{mean} = 1.57 \pm 0.34$, p = 0.408) for the 12-month interval.

NAA at 12-month interval

Similar to the 6-month interval data, neither the NAWM groups nor the Lesion groups showed significant differences within the groups for NAA/Cr ratios.

Point Spread Function effect

Some of the NAWM voxels that developed lesions during the 6-month interval were located near voxels that already contained lesion. In order to evaluate the effect of point spread function on our data, we calculated the lesion load found in the adjacent voxels and found no correlation between Cho/Cr or NAA/Cr in NL voxels and surrounding lesion volume ($r = 0.035$, $p = 0.787$ and $r = -0.121$, $p = 0.349$, respectively). We repeated the same analysis for the NAWM voxels that remained stable during the 6-month interval and again found no correlation between Cho/Cr or NAA/Cr in NN voxels and adjacent lesion volume ($r = -0.104$, $p = 0.576$ and $r = 0.101$, $p = 0.587$, respectively).

Discussion

Our results demonstrate that Cho/Cr ratios are elevated in areas of as NAWM that develop MRI-visible lesions 6 months and/or 12 months later, compared with areas that remain NAWM. We also found Cho/Cr to be elevated in Lesion voxels that increased in lesion content at the 6-month scan versus those that remained stable. The pathophysiological significance of an elevated Cho has been attributed to active demyelination and inflammation. The observed elevated Cho/Cr in NAWM that subsequently develops a plaque suggests that there is prior to the lesion becoming detectable by conventional MRI, an early stage in lesion formation. This could be associated with physico-chemical change in myelin, either prior to or associated with inflammation [4].

Although both Lesion voxel groups displayed a higher Cho/Cr than the NAWM that remained stable, the active plaque group had a higher Cho/Cr than the stable plaque group. This suggests that there are two different processes that lead to an elevated Cho/Cr. The first is demyelination, which is most likely common to both Lesion voxel groups. The second is inflammation, which is probably superimposed on the myelin abnormality.

We attribute the lower Cho/Cr ratio observed in the stable voxel groups compared with the unstable voxel groups to a lower Cho and not a higher Cr. This is highly probable since NAA/Cr was not significantly different between the two groups. Absolute quantitation of metabolites with *in vivo* MRS studies requires T1 and T2 relaxation time weighting of the spectra which may be difficult to assess in pathological tissue [12].

The significance of Cho has been studied in various other pathologies, Miller et al. [15], in looking at neoplasms and brain infections, found that free choline, phosphorylcholine, glycerylphosphorylcholine, as well as tissue cellularity correlated with the ^{1}H-MRS Cho peak. An in vitro ^{1}H-MRS study done on EAE animals found free choline, phosphorylcholine and betaine as the main determinants of the Cho peak [4]. The significance of betaine is controversial since it is not known if this compound exists in the human brain. The authors do mention that betaine is elevated in cultured peritoneal macrophages that have been incubated with myelin and have degraded it. This would suggest that the enzyme required to produce this compound may be carried into the CNS via inflammatory cells. Neuropathological studies done on MS patients revealed that inflammatory cells are not always present in areas of active demyelination [13, 23]. These results suggest that perivenous inflammation and demyelination may be, to some extent, separate pathological processes.

There is now growing evidence that activated T cells can cross an intact BBB and subsequently leave if they do not encounter an antigen [10]. If they do encounter an antigen they initiate an inflammatory cascade involving various cytokines that cause changes in the endothelium and lead to the recruitment of more inflammatory cells and activation of microglia. It may be speculated that a regional increase of Cho/Cr in the NAWM that subsequently develops plaque may be associated with this early inflammatory process.

It has been suggested that aside from the axonal damage occurring in the NAWM of MS patients, there is a proliferation of glial cells yielding an increase in Cr [29]. Since we look at ratios, this might be proposed as an explanation for the lower Cho/Cr in the NAWM versus the lesions. However, in the current study, we found that the NAWM that develops plaques actually has a high Cho/Cr. Thus one would have to propose that gliosis only occurs in the stable NAWM which had the lowest Cho/Cr ratio and this does not seem likely.

In a postmortem study, Davies et al. [5] demonstrated that Cr is decreased in chronic plaques and in voxels adjacent to plaques as compared with normal controls. A change in Cr is unlikely to be responsible for the results seen in this study because both stable and unstable NAWM voxels lay adjacent to some voxels containing lesions and the comparison was between these groups not with normal controls. In addition, there is little plaque volume in our spectroscopic VOI and no correlation was found between Cho/Cr or NAA/Cr and adjacent lesion volume for the NN or NL groups. Furthermore, if one looks at the stable and unstable Lesion voxels, one notices that Cho/Cr is higher in lesion voxels that increase in size, indicating a more active lesion, as compared with the lesion voxels that stay the same. If the chronic plaques had a lower Cr as proposed by Davies et al. [5]

then the stable lesion voxel group should have shown the higher Cho/Cr ratio.

The results of this study imply that pre-lesional changes in myelin with or without associated inflammation may be sufficient to produce elevated Cho/Cr ratios without any associated demyelination. We hypothesize that there may be MRI-invisible inflammation going on in the NAWM long before a plaque develops. Our study shows that even a year before a plaque develops the NAWM of that area shows an elevated Cho/Cr. Such evidence would further support the rationale for targeting MS therapies at preventing damage in the NAWM by reducing inflammation.

Acknowledgements This study was supported by grants from the Medical Research Council of Canada and the MS Society of Canada. The authors gratefully acknowledge the excellent technical support during MRS studies of Mr. Gilles Leroux, Mr. Andre Cormier, Ms. Caroline Hurst, Mr. Jeff Fieldsend, Mr. Marc Lemieux and Mr. Philip Lewis. We also acknowledge the support of Ms. Ellie Tobman in coordinating the subjects. We are grateful to all the study participants for their time and cooperation.

References

1. Arnold D, Narayanan S, De Stefano N, Reddy H, Matthews PM (2001) Magnetic Resonance Spectroscopy of Multiple Sclerosis: Imaging Axonal Damage. In: Multiple Sclerosis: Tissue Destruction and Repair. Kappos L, Kesselring J, Radu EW, Johnson K (eds) London: Martin Duntz Ltd, pp 77–90
2. Arnold DL, Matthews PM, Francis G, Antel J (1990) Proton magnetic resonance spectroscopy of human brain in vivo in the evaluation of multiple sclerosis: assessment of the load of disease. Magn Reson Med 14 (1): 154–159
3. Arnold DL, Matthews PM, Francis GS, O'Connor J, Antel JP (1992) Proton magnetic resonance spectroscopic imaging for metabolic characterization of demyelinating plaques. Ann Neurol 31 (3): 235–241
4. Brenner RE, Munro PM, Williams SC, Bell JD, Barker GJ, Hawkins CP, et al. (1993) The proton NMR spectrum in acute EAE: the significance of the change in the Cho:Cr ratio. Magn Reson Med 29 (6): 737–745
5. Davies SE, Newcombe J, Williams SR, McDonald WI, Clark JB (1995) High resolution proton NMR spectroscopy of multiple sclerosis lesions. J Neurochem 64 (2): 742–748
6. den Hollander JA OB, van Vroonhoven H, Luyten PR (1991) Elimination of magnetic field distortions in 1H NMR spectroscopic imaging [abstract]. Proc Soc Magn Reson Med 1: 472
7. Filippi M, Rocca MA, Martino G, Horsfield MA, Comi G (1998) Magnetization transfer changes in the normal appearing white matter precede the appearance of enhancing lesions in patients with multiple sclerosis. Ann Neurol 43 (6): 809–814
8. Goodkin DE, Rooney WD, Sloan R, Bacchetti P, Gee L, Vermathen M, et al. (1998) A serial study of new MS lesions and the white matter from which they arise. Neurology 51 (6): 1689–1697
9. Gupta RK, Sinha U, Cloughesy TF, Alger JR (1999) Inverse correlation between choline magnetic resonance spectroscopy signal intensity and the apparent diffusion coefficient in human glioma. Magn Reson Med 41 (1): 2–7
10. Hickey WF (1991) Migration of hematogenous cells through the blood-brain barrier and the initiation of CNS inflammation. Brain Pathol 1 (2): 97–105
11. Husted CA, Goodin DS, Hugg JW, Maudsley AA, Tsuruda JS, de Bie SH, et al. (1994) Biochemical alterations in multiple sclerosis lesions and normal-appearing white matter detected by in vivo 31P and 1H spectroscopic imaging. Ann Neurol 36 (2): 157–165
12. in 't Zandt H, van Der Graaf M, Heerschap A (2001) Common processing of in vivo MR spectra. NMR Biomed 14 (4): 224–232
13. Lucchinetti CF, Bruck W, Rodriguez M, Lassmann H (1996) Distinct patterns of multiple sclerosis pathology indicates heterogeneity on pathogenesis. Brain Pathol 6 (3): 259–274
14. Matthews PM, Francis G, Antel J, Arnold DL (1991) Proton magnetic resonance spectroscopy for metabolic characterization of plaques in multiple sclerosis [published erratum appears in Neurology Nov, 41 (11): 1828]. Neurology 41 (8): 1251–1256
15. Miller BL, Chang L, Booth R, Ernst T, Cornford M, Nikas D, et al. (1996) In vivo 1H MRS choline: correlation with in vitro chemistry/histology. Life Sci 58 (22): 1929–1935
16. Miller DH, Grossman RI, Reingold SC, McFarland HF (1998) The role of magnetic resonance techniques in understanding and managing multiple sclerosis. Brain 121 (Pt 1): 3–24
17. Miller DH, Albert PS, Barkhof F, Francis G, Frank JA, Hodgkinson S, et al. (1996) Guidelines for the use of magnetic resonance techniques in monitoring the treatment of multiple sclerosis. US National MS Society Task Force. Ann Neurol 39 (1): 6–16
18. Narayana PA, Doyle TJ, Lai D, Wolinsky JS (1998) Serial proton magnetic resonance spectroscopic imaging, contrast-enhanced magnetic resonance imaging, and quantitative lesion volumetry in multiple sclerosis. Ann Neurol 43 (1): 56–71
19. Ordidge RJ, Mansfield P, Lohman JA, Prime SB (1987) Volume selection using gradients and selective pulses. Ann N Y Acad Sci 508: 376–385
20. Pan JW, Hetherington HP, Vaughan JT, Mitchell G, Pohost GM, Whitaker JN (1996) Evaluation of multiple sclerosis by 1H spectroscopic imaging at 4.1 T. Magn Reson Med 36 (1): 72–77
21. Pike GB, De Stefano N, Narayanan S, Worsley KJ, Pelletier D, Francis GS, et al. (2000) Multiple sclerosis: magnetization transfer MR imaging of white matter before lesion appearance on T2-weighted images. Radiology 215 (3): 824–830
22. Richards TL (1991) Proton MR spectroscopy in multiple sclerosis: value in establishing diagnosis, monitoring progression, and evaluating therapy. AJR Am J Roentgenol 157 (5): 1073–1078
23. Rodriguez M, Scheithauer B (1994) Ultrastructure of multiple sclerosis. Ultrastruct Pathol 18 (1–2): 3–13
24. Rooney WD, Goodkin DE, Schuff N, Meyerhoff DJ, Norman D, Weiner MW (1997) 1H MRSI of normal appearing white matter in multiple sclerosis. Mult Scler 3 (4): 231–237
25. Sarchielli P, Presciutti O, Pelliccioli GP, Tarducci R, Gobbi G, Chiarini P, et al. (1999) Absolute quantification of brain metabolites by proton magnetic resonance spectroscopy in normal-appearing white matter of multiple sclerosis patients. Brain 122 (Pt 3): 513–521
26. Simmons ML, Frondoza CG, Coyle JT (1991) Immunocytochemical localization of N-acetyl-aspartate with monoclonal antibodies. Neuroscience 45 (1): 37–45

27. Stewart WA, Hall LD, Berry K, Paty DW (1984) Correlation between NMR scan and brain slice data in multiple sclerosis [letter]. Lancet 2 (8399): 412

28. Trapp BD, Peterson J, Ransohoff RM, Rudick R, Mork S, Bo L (1998) Axonal transection in the lesions of multiple sclerosis [see comments]. N Engl J Med 338 (5): 278–285

29. van Walderveen MA, Barkhof F, Pouwels PJ, van Schijndel RA, Polman CH, Castelijns JA (1999) Neuronal damage in T1-hypointense multiple sclerosis lesions demonstrated in vivo using proton magnetic resonance spectroscopy. Ann Neurol 46 (1): 79–87